eLIFE
elifesciences.org

Figures and figure supplements

Engineered proteins detect spontaneous DNA breakage in human and bacterial cells

Chandan Shee, et al.

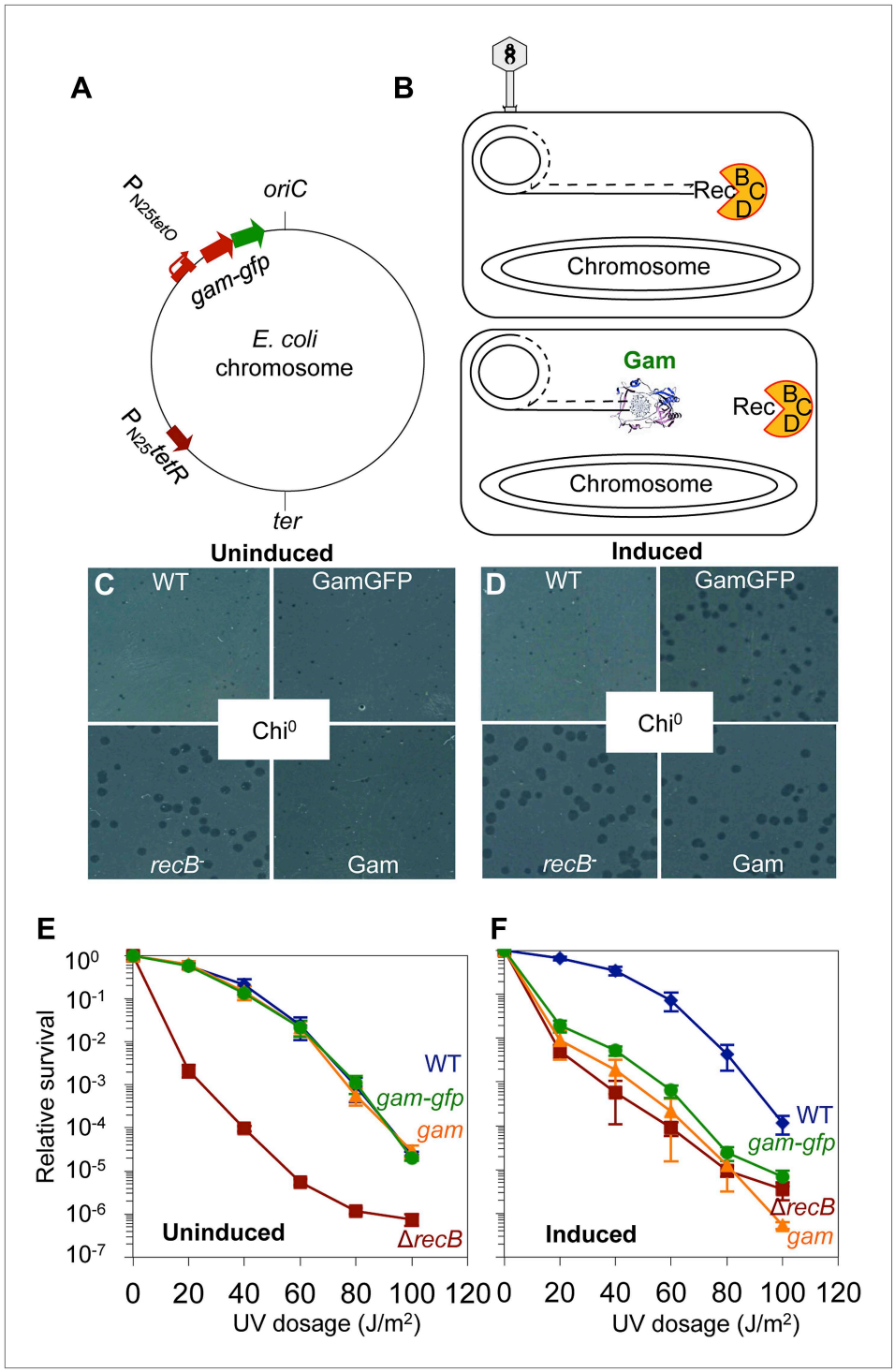

Figure 1. GamGFP production mimics *recB* double-strand-exonuclease defect. (**A**) Doxycycline-inducible *gam-gfp* fusion construct in the *E. coli* chromosome. Constitutively produced TetR protein represses the $P_{N25tetO}$ promoter, which produces GamGFP upon doxycycline induction. *oriC*, origin of replication; *ter*, replication terminus; arrows, directions of transcription. (**B**) Phage λ assay for end-blocking activity by Mu Gam and GamGFP. Rolling-circle replication of phage λ*red gam* is inhibited by *E. coli* RecBCD, which causes small plaques of λ*red gam* on wild-type *E. coli* (***Smith, 1983***). Mu Gam protein binds and protects DNA ends from RecBCD exonuclease activity (***Akroyd and Symonds, 1986***) and so is expected to allow rolling-circle replication of λ*red gam* and therefore allow formation of large plaques. (**C**) λ*red gam* plaques are small on *recB*$^+$ (WT) and large on *recB*-deficient cells (*recB*$^-$).

Figure 1. Continued on next page

Figure 1. Continued

Plaques produced on WT cells carrying *gam* and *gam-gfp* are small when Gam and GamGFP proteins are not produced (Uninduced). (**D**) λ*red gam* produce large plaques on WT cells if Gam or GamGFP are produced (Induced). (**E**) UV sensitivity of *E. coli recB*-null mutant compared with *recB*$^{+}$(WT), and uninduced *gam* and *gam-gfp* carrying cells. WT (♦), *recB*$^{-}$ (■), WT GamGFP, (●); WT Gam, (▲). (**F**) Induction of Gam or GamGFP with 200 ng/ml doxycycline causes UV sensitivity similar to that of *recB*-null mutant cells, indicating that Gam or GamGFP block RecBCD action on double-stranded DNA ends. WT, SMR14327; *recB*, SMR8350; WT GamGFP, SMR14334; WT Gam, SMR14333. Representative experiment performed three times with comparable results.

DOI: 10.7554/eLife.01222.003

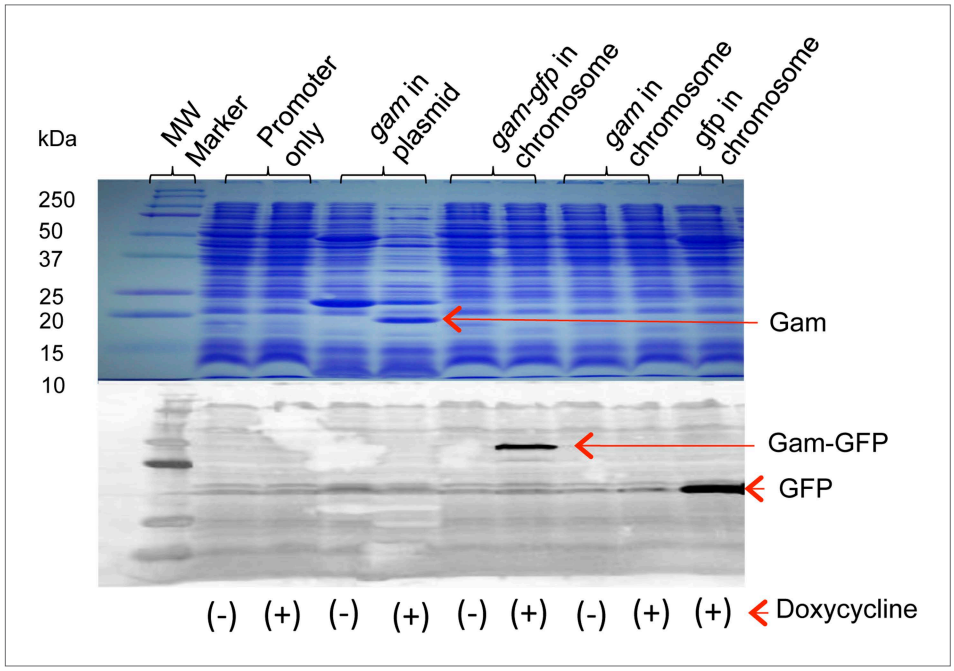

Figure 1—figure supplement 1. Production of Gam and GamGFP fusion proteins in *E. coli*. Doxycycline induction and detection of plasmid-borne Gam and chromosomally encoded GamGFP and GFP are performed by Coomassie blue staining following electrophoresis (Gam) or by western blot immunodetection (GamGFP, GFP), in upper and lower panels, respectively. Cultures grown, as described in 'Materials and methods', were incubated in the presence or absence (+ or −) of 100 ng/ml doxycycline. For the western blot, protein was visualized using antibodies against GFP. Arrows indicate positions of Gam, GFP, and GamGFP within the gel. Molecular weights of protein standards are indicated to left. Strains are: promoter only, SMR14311; *gam* in plasmid, SMR13908; chromosomal *gam-gfp*, SMR14334; chromosomal *gam*, SMR14333; and chromosomal *gfp*, SMR14332.

DOI: 10.7554/eLife.01222.004

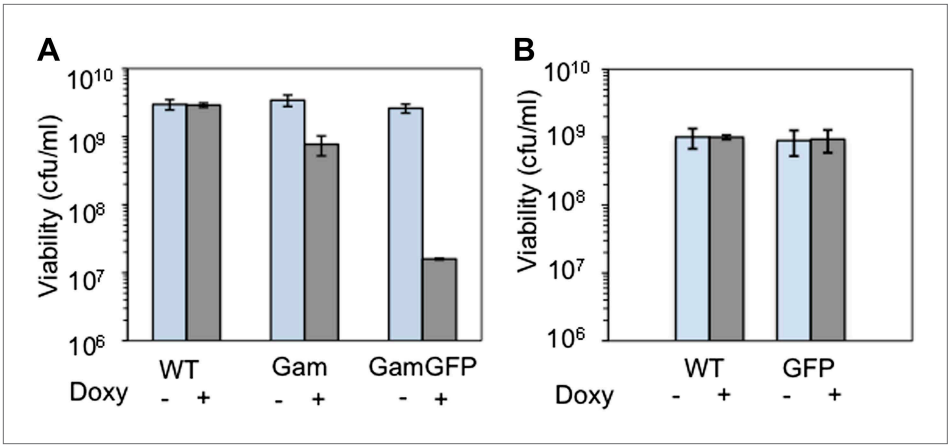

Figure 1—figure supplement 2. Long-term GamGFP production reduces *E. coli* viability. Greater viability loss with GamGFP than Gam implies that GamGFP is a superior DSE trap. (**A**) We quantified the effect of long-term Gam and GamGFP production on cell viability by inducing Gam or GamGFP production briefly in split log-phase cultures, then plating them for viable colony-forming units (cfu) on inducing or non-inducing solid medium with long-term overnight incubation. Saturated LBH cultures of SMR14327 (WT), SMR14333 (Gam) and SMR14334 (GamGFP) were diluted 1:100 in fresh LBH medium and grown shaking at 37°C for 90 min, then either induced with 200 ng/ml of doxycycline or not, and grown for an additional 2 hours shaking at 37°C prior to plating for cfu on LBH solid medium with or without 200 ng/ml doxycycline. The colonies were scored after overnight incubation at 37°C. We observe that induced cultures of the Gam- and GamGFP-producing strains show, respectively, 32 ± 9% and 0.47 ± 0.06% the number of viable cfu as either WT cells with no *gam* gene or uninduced *gam*- or *gam-gfp*-containing cells (mean ± SD, three experiments). These data imply that DSBs bound by GamGFP are not repaired or are repaired inefficiently. Whereas the viability of Gam producers is similar to that of liquid cultures of *E. coli recBC* DSB-repair-defective cells, which typically contain ~30% viable cells (e.g., ***Miranda and Kuzminov, 2003***), GamGFP producers have lower viability. These data suggest that GamGFP is a more permanent DSE-trap and blocker of repair than Gam is, and that there is residual RecBC-independent DSB repair in *recBC*-defective cells. We speculate that the GFP moiety might confer more permanence to the GamGFP binding of DSBs either because the GamGFP protein inherently possesses a reduced dissociation constant or perhaps because the GFP moiety instigates multimerization with other GFP moieties in other GamGFP molecules present in the cell. This could both confer its outstanding focus-forming ability and might additionally retard end dissociation. (**B**) We find no cfu-reducing effect of production of GFP alone.

DOI: 10.7554/eLife.01222.005

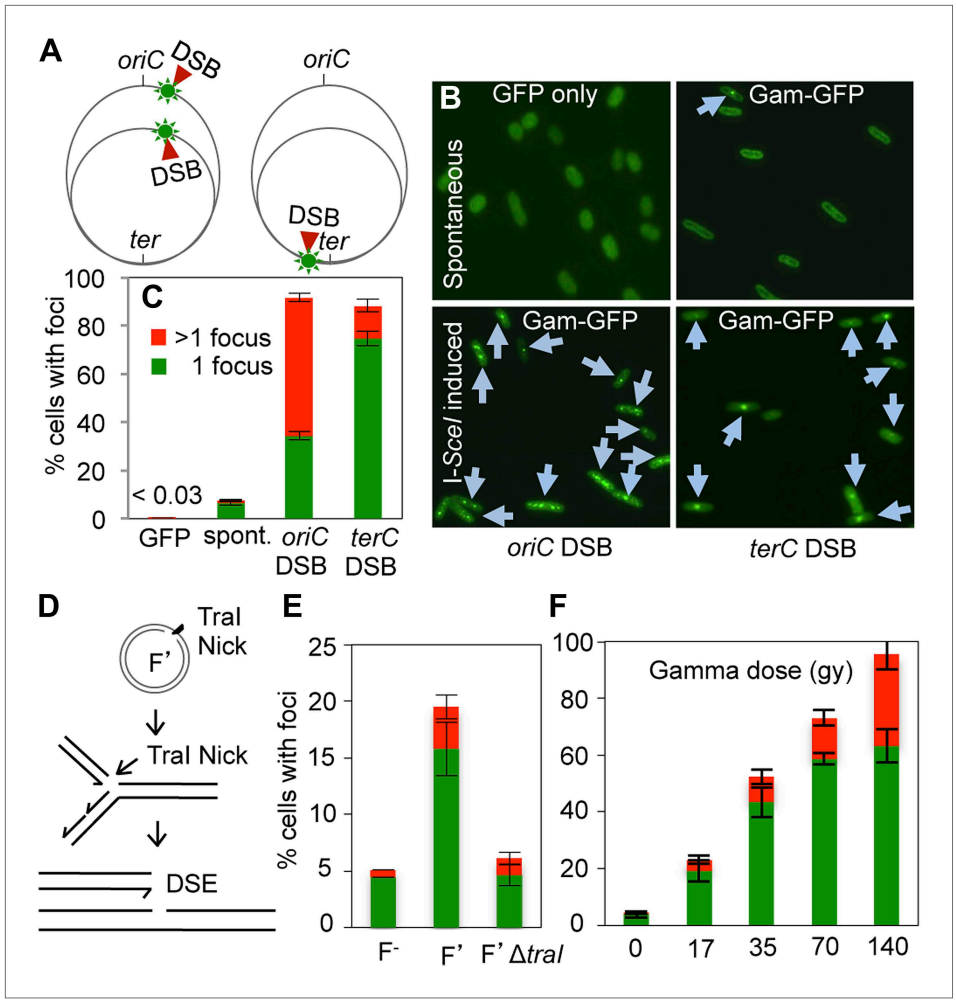

Figure 2. GamGFP foci at DSBs in living *E. coli*. (**A**) Strategy. In log-phase replicating *E. coli*, cells have more copies of origin (*oriC*)-proximal than terminus (*ter*)-proximal DNA and so will have more DSBs per cell when cleaved by chromosomally encoded I-*Sce*I (***Ponder et al., 2005***) at a cutsite (red arrow/green flash) near *ori* than near *ter*. (**B**) Representative data (arrows indicate foci). (**C**) Quantification from multiple experiments shows correlation of GamGFP foci with numbers of DSBs per cell. Cells have >1 focus when cleaved by I-*Sce*I near *ori*, usually 1 focus per cell when cleaved by I-*Sce*I near *ter*, far fewer cells with foci when only spontaneous DSBs are present (no I-*Sce*I cleavage), and <0.03% of cells with foci when GFP alone is produced. *E. coli* strains: GFP only, SMR14332; GamGFP, SMR14350; *oriC* DSB, SMR14354; *ter* DSB, SMR14362. Error bars, ± SEM. (**D**) Strategy: a site-specific ssDNA nick made by TraI ssDNA endonuclease at *oriT* in the F plasmid becomes a one-ended DSB upon replication by fork collapse (***Kuzminov, 2001***). (**E**) TraI-dependent GamGFP foci imply that GamGFP detects one-ended DSBs. Cells with no F plasmid (F^-), an F′ plasmid encoding TraI (F′), or an isogenic *traI*-deleted F′ (F′Δ*traI*): strains SMR14015, SMR16387, and SMR16475. (**F**) GamGFP foci are correlated with dose of DSB-producing γ-radiation. ***Figure 2—figure supplement 2A*** shows linear correlation of foci with dose. Strain, SMR14350. Cells with 1 focus, green; >1 focus, red.

DOI: 10.7554/eLife.01222.006

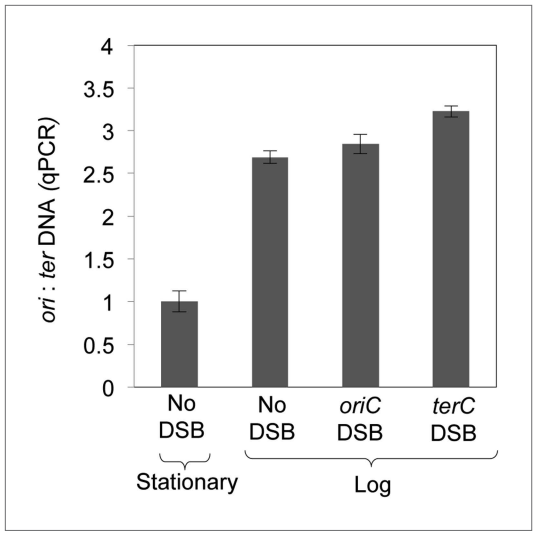

Figure 2—figure supplement 1. Quantitative real-time PCR shows ~three-fold more DNA copies near *ori* than *ter* in log-phase, regardless of I-*Sce*I cleavage, implying that some cells have two and some have four *ori*:*ter* regions.

DOI: 10.7554/eLife.01222.007

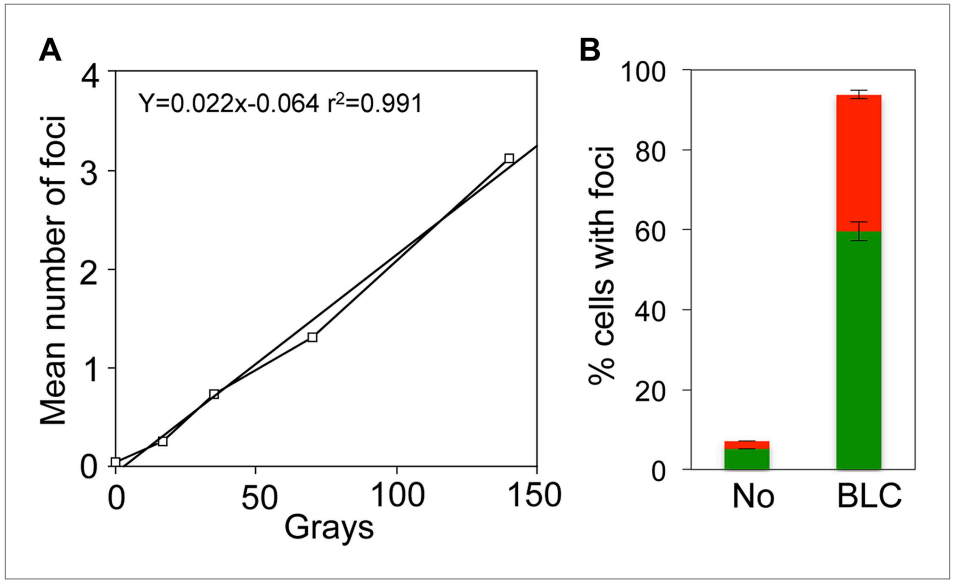

Figure 2—figure supplement 2. Linear gamma-ray dose-response and bleomycin induction of GamGFP foci in *E. coli*. (**A**) Numbers of GamGFP foci are linearly correlated with dose of DSB-producing γ-irradiation. Numbers of foci at different doses of γ-irradiation were calculated from the data displayed in ***Figure 2F***. (**B**) GamGFP foci form in response to bleomycin induced DSBs in living *E. coli*. Twenty μg/ml bleomycin (BLC) promotes GamGFP foci. Green, 1 focus per cell; red, >1 focus per cell.

DOI: 10.7554/eLife.01222.008

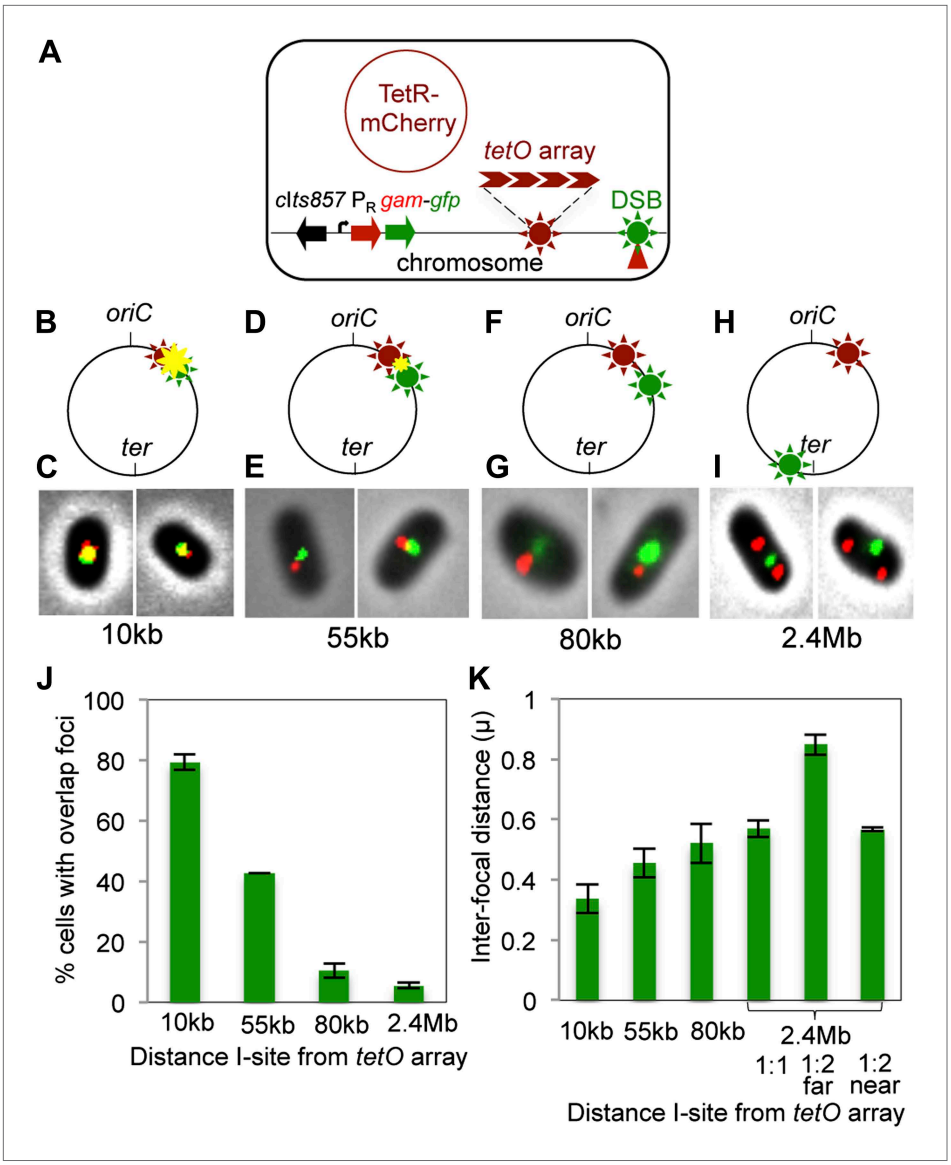

Figure 3. Subcellular/subgenomic localization of DSBs in living *E. coli*. (**A**) Strategy: we varied the location of I-*Sce*I cleavage sites (I-sites) in different strains relative to a fixed-position chromosomal TetR-mCherry-bound *tetO* array, with GamGFP temperature inducibly produced from chromosomal λP_R (*cIts857* P_R*gam-gfp*). Red circle, plasmid that produces TetRmCherry. (**B**–**H**) Diagrams of *E. coli* chromosomes with inducible I-*Sce*I endonuclease and I-sites engineered (**B**) 10 kb, (**D**) 55 kb, (**F**) 80 kb, and (**H**) 2.4 Mb from the *tetO* array. Co-localization of TetR-mCherry (*) and GamGFP foci (*) results in a yellow focus (*). (**C**, **E**, **G**, **I**) Representative fluorescence microscopy results show co-localization of mCherry and GamGFP (yellow foci) at 10 kb (**C**), and non-overlapping foci at 55 kb (**E**), 80 kb (**G**), 2.4 Mb (**I**) in strains SMR16600, SMR16711, SMR16713, and SMR16606. (**J**) Percentage of cells with yellow overlapped foci at each distance. (**K**) Mean interfocal distances. At 2.4 Mb, there were frequently two red foci per one green focus, reflecting more copies of *ori*- than *ter*-proximal DNA during replication. The greater interfocal distance (far) is plotted separately from the shorter (near), and cells with 1:1 ratios were counted separately. Data represent three independent experiments, error bars indicate SEM, with the number of cells counted in all three totaling: 298, 10 kb; 204, 55 kb; 333, 80 kb; and 1347, 2.4 Mb.

DOI: 10.7554/eLife.01222.009

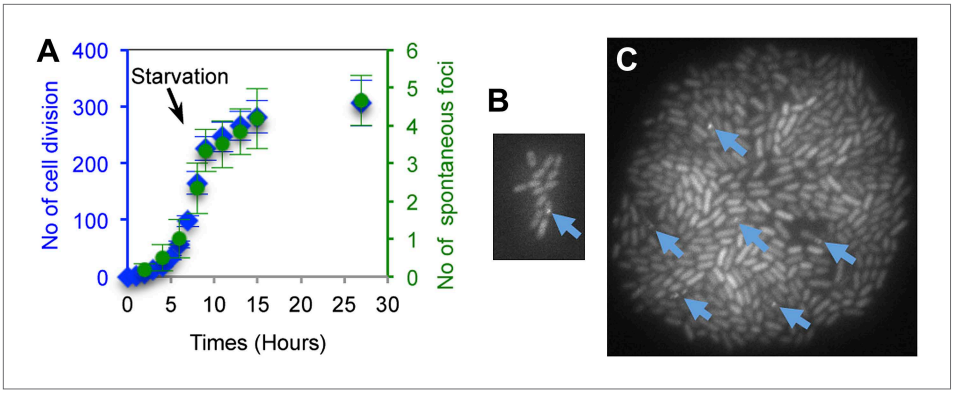

Figure 4. Generation-dependence of spontaneous GamGFP focus formation in proliferating *E. coli*. Log-phase GamGFP-pre-induced cells were loaded into a microfluidic chamber in which single cells anchor then divide to form single-cell-layer microcolonies. The numbers of cell divisions and appearance of spontaneous foci were captured with time-lapse photography. Rapid growth in glucose during the first 9 hr was followed by washing cells in the same medium lacking glucose for 18 hr to slow and halt cell divisions. (**A**) Spontaneous DSB foci are correlated with numbers of cell divisions. Summary of data for six cells that became microcolonies. Blue (♦), number of cell divisions; green (●), cumulative number of spontaneous foci that appear in each microfluidics micro-colony (mean ± SEM, six microcolonies). (**B**) Representative 2-hr micro-colony with a GamGFP focus (arrow). (**C**) Representative 15-hr micro-colony with GamGFP foci (arrows).

DOI: 10.7554/eLife.01222.010

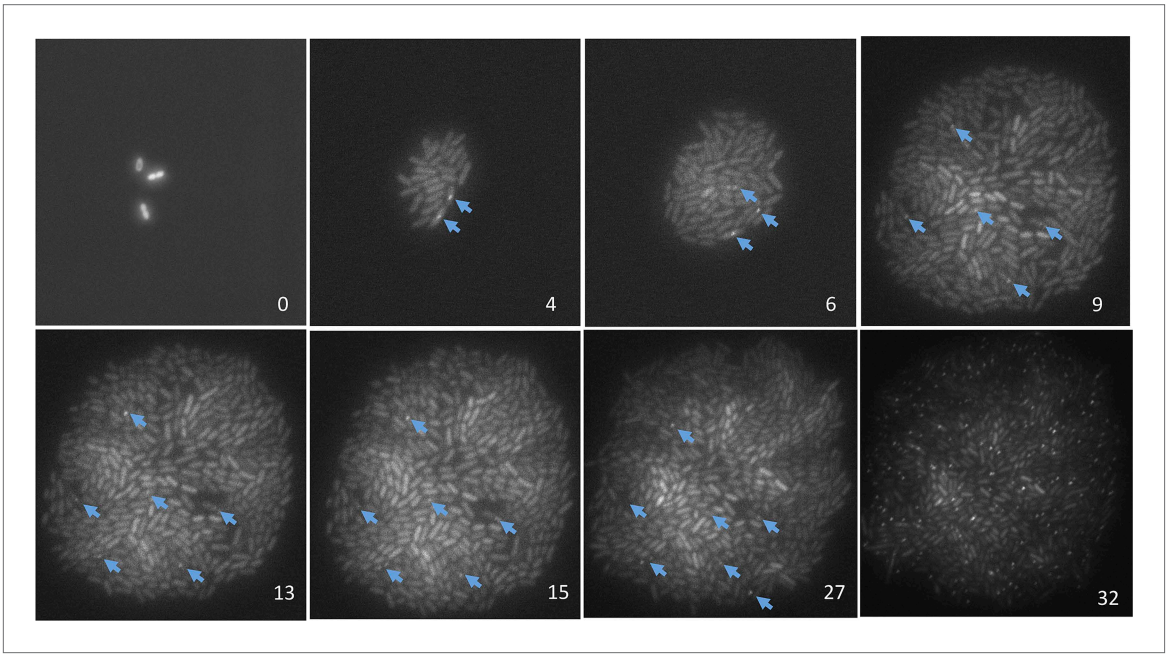

Figure 4—figure supplement 1. Representative data on the origins of spontaneous DSBs over time during growth, or growth retardation, visualized and quantified per 'Materials and methods', Microfluidics and time-lapse fluorescence microscopy of *E. coli*. Numbers in the lower right of each frame are hours after loading into the microfluidic chamber. GamGFP foci are indicated with arrows. Note that cells expressing *gam-gfp* show variation in the amount of GFP per cell documented for *E. coli* (***Elowitz et al., 2002***) and other cells expressing any fluorescent-protein gene. This variation represents stochastic variation in transcription and mRNA accumulation, but the data scored are foci (arrows). Cells were bathed in medium with glucose for 9 hr to allow log-phase growth, then cell divisions slowed and ultimately halted (***Figure 4A***) by switching to the same medium without glucose. Then at 27 hr, 20 μg/ml phleomycin was added to induce DSBs, visible as foci in 45± 5% of cells at 32 hr, to verify that had DSBs formed in the starving cells, they would have been visible as foci. These images were taken under very low-dose (30 ms) exposure to fluorescent light to minimize fluorescence-induced DNA damage (***Ge et al., 2013***) and possible induction of GamGFP foci. Control experiments summarized in 'Materials and methods' show that these brief pulses did not induce GamGFP foci (Microfluidics and time-lapse microscopy of *E. coli*, 'Evidence that fluorescence exposure did not contribute to the spontaneous GamGFP foci scored)'.

DOI: 10.7554/eLife.01222.011

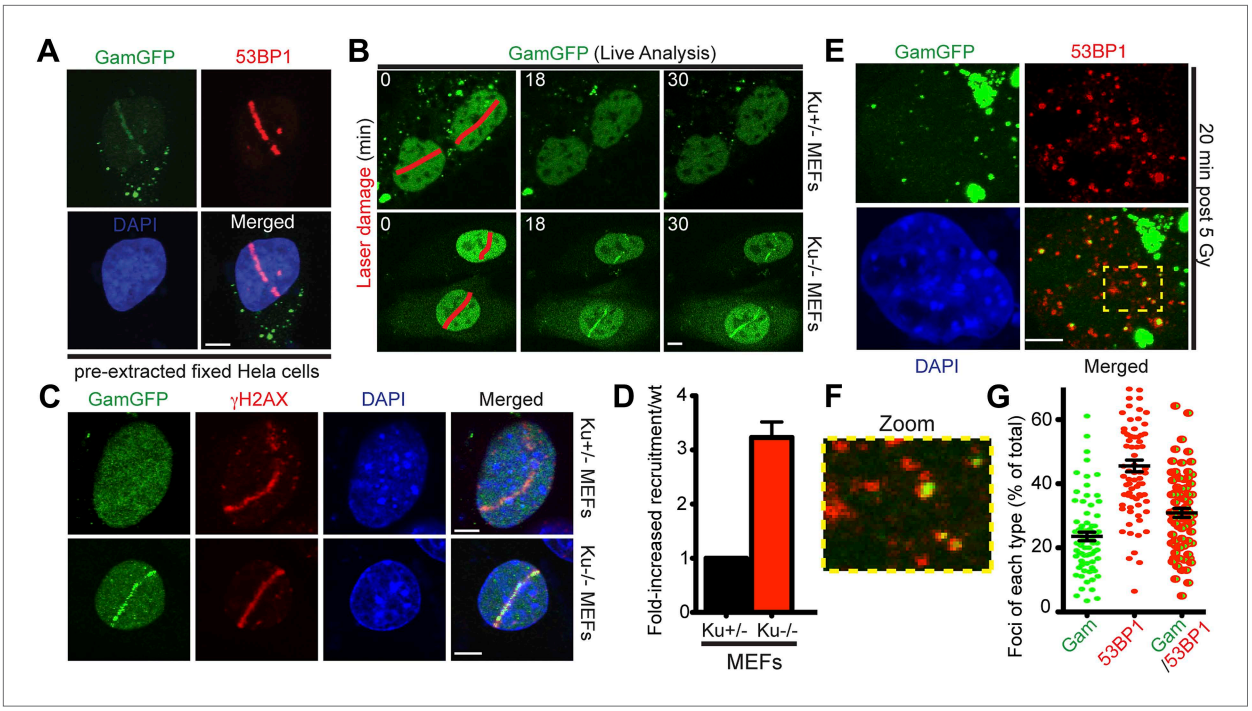

Figure 5. GamGFP marks DSBs in mammalian cells and is inhibited by Ku. (**A**) GamGFP co-localizes with 53BP1 on laser-induced DNA breaks. (**B**) Ku inhibits recruitment of GamGFP to laser-induced damage, live cells. (**C** and **D**) Ku inhibits recruitment of GamGFP, fixed cells. Mean ± SEM of three experiments, n >25 cells each. (**E**) GamGFP forms IR-induced foci in Ku80-defective MEFs. (**F**) Zoomed image from **E**. (**G**) IR-induced foci containing Gam only, 53BP1 only or both Gam and 53BP1 (>2600 total foci counted in three independent experiments). Error bars, SEM. Scale bars = 5 μm.

DOI: 10.7554/eLife.01222.012

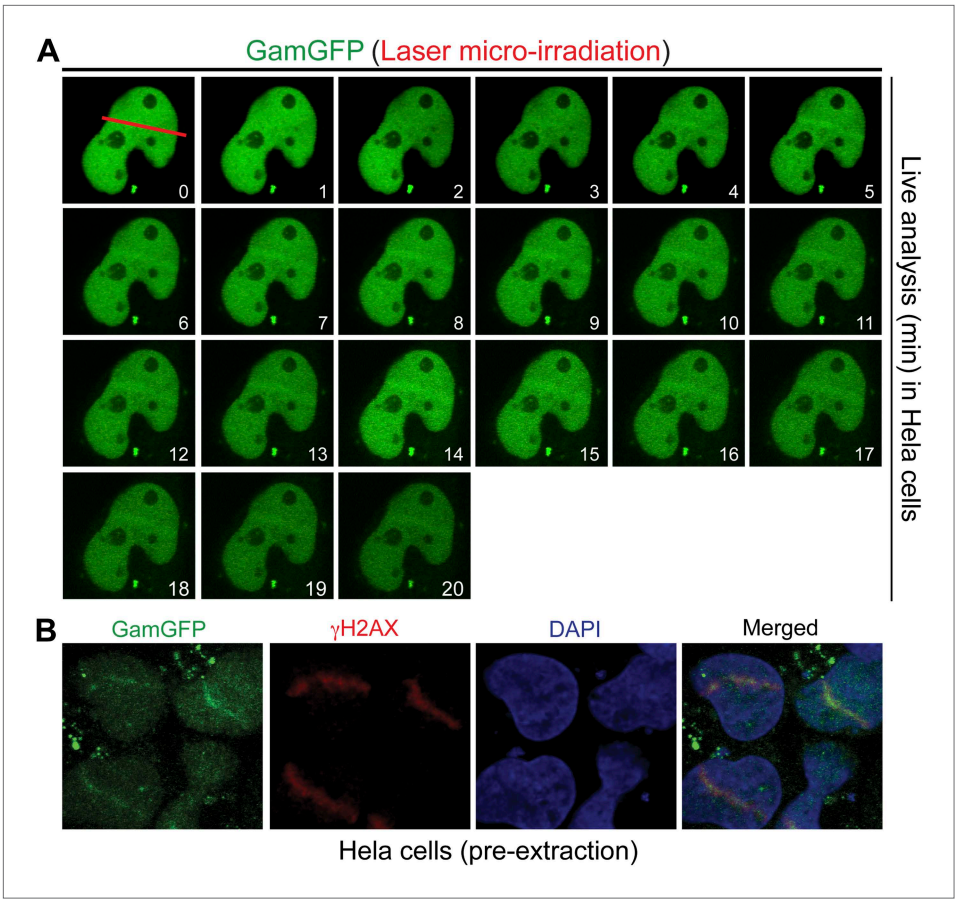

Figure 5—figure supplement 1. GamGFP marks DSBs in mammalian cells. (**A**) Live analysis of GamGFP localization to laser-induced DNA damage. Hela cells producing GamGFP were laser damaged along the cell track indicated by the red line at 0 min (m) and images were taken at the indicated times as shown. (**B**) GamGFP co-localizes with γH2AX in fixed Hela cells.

DOI: 10.7554/eLife.01222.013

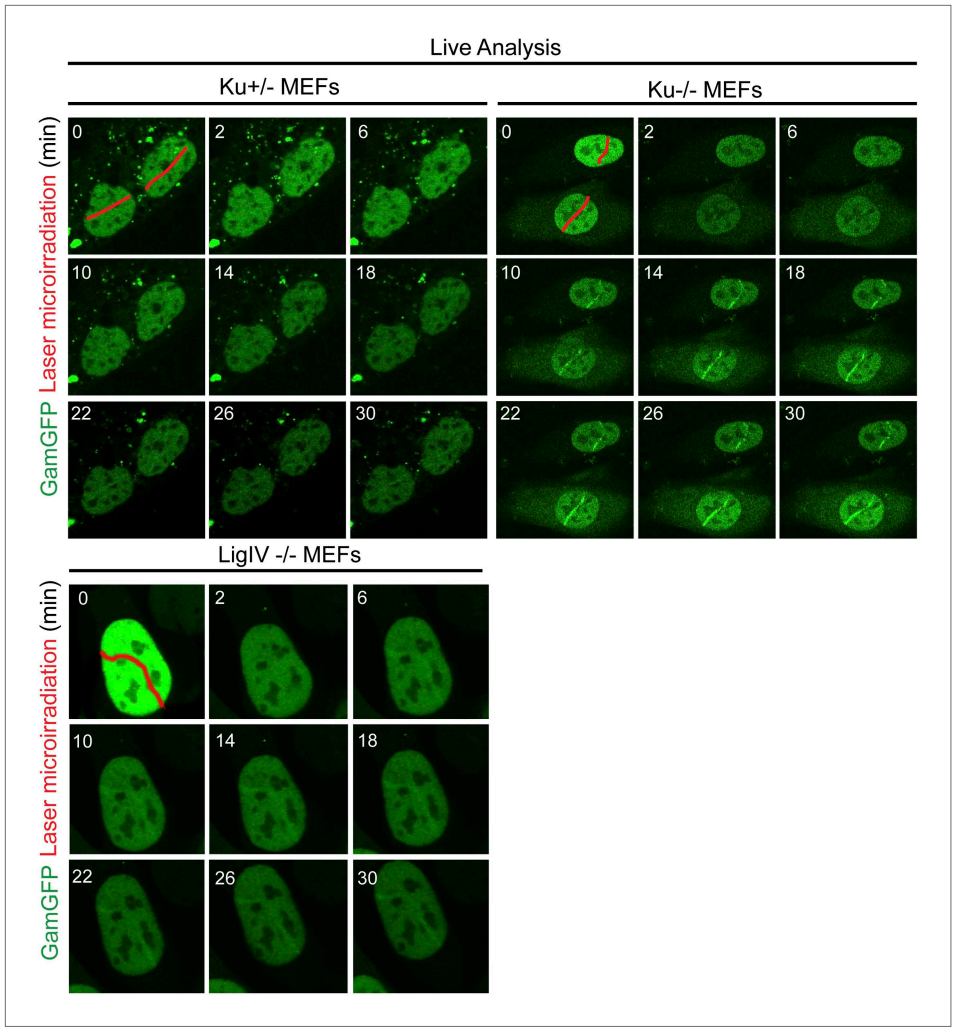

Figure 5—figure supplement 2. Ku inhibits GamGFP recruitment at DSBs independently of non-homologous end joining. Cells lacking either Ku80 or LigIV are defective in non-homologous end joining (NHEJ), yet the presence of Ku still inhibits recruitment of GamGFP to laser-induced DSBs even in NHEJ-defective cells, and thus independently of the cell's ability to complete NHEJ. Whereas it could have been possible that reduced GamGFP recruitment in the presence of Ku was caused by reduced persistence of DSBs due to their repair by NHEJ, our data show instead that Ku inhibits recruitment independently of successful NHEJ and imply that Ku binding to DSEs itself is inhibitory.

DOI: 10.7554/eLife.01222.014

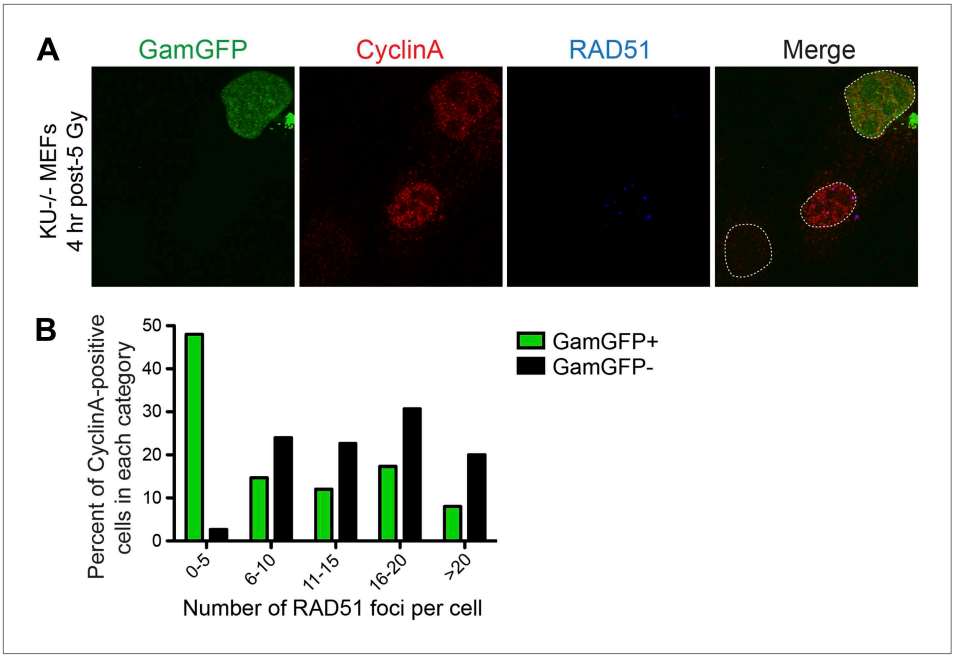

Figure 6. GamGFP inhibits IR-induced RAD51 foci, apparently blocking end resection. We quantified RAD51 foci (single-stranded DNA) (***Raderschall et al., 1999***) induced by IR, so presumably at DSBs, in S-G2 (CyclinA-positive) cells that either did or did not produce GamGFP, from the same transfections. (**A**) The GamGFP-positive Ku80-defective MEFs display reduced RAD51 foci upon IR treatment in S/G2 cells. Cells were analyzed by immunofluorescence with the indicated antibodies. S/G2 cells were identified by positive staining of CyclinA. Dotted white lines mark cell nuclei. (**B**) Quantification of RAD51 foci in CyclinA-positive cells with or without GamGFP production (cumulative values from three experiments with >75 cells total). Each cell is 'Z-stacked' (optically sectioned) so that all RAD51 foci were examined. The data indicate that most GamGFP-positive cells have few (0–5) RAD51 foci per cell, and that those cells with more RAD51 foci (classes 6–10, 11–15, 16–20 and >20) are enriched among the GamGFP-negative cells. These data indicate a partial mutual exclusivity of GamGFP presence and RAD51 foci, as would be expected if Gam binding to DSEs blocks the resection that creates the ssDNA onto which RAD51 binds.
DOI: 10.7554/eLife.01222.015

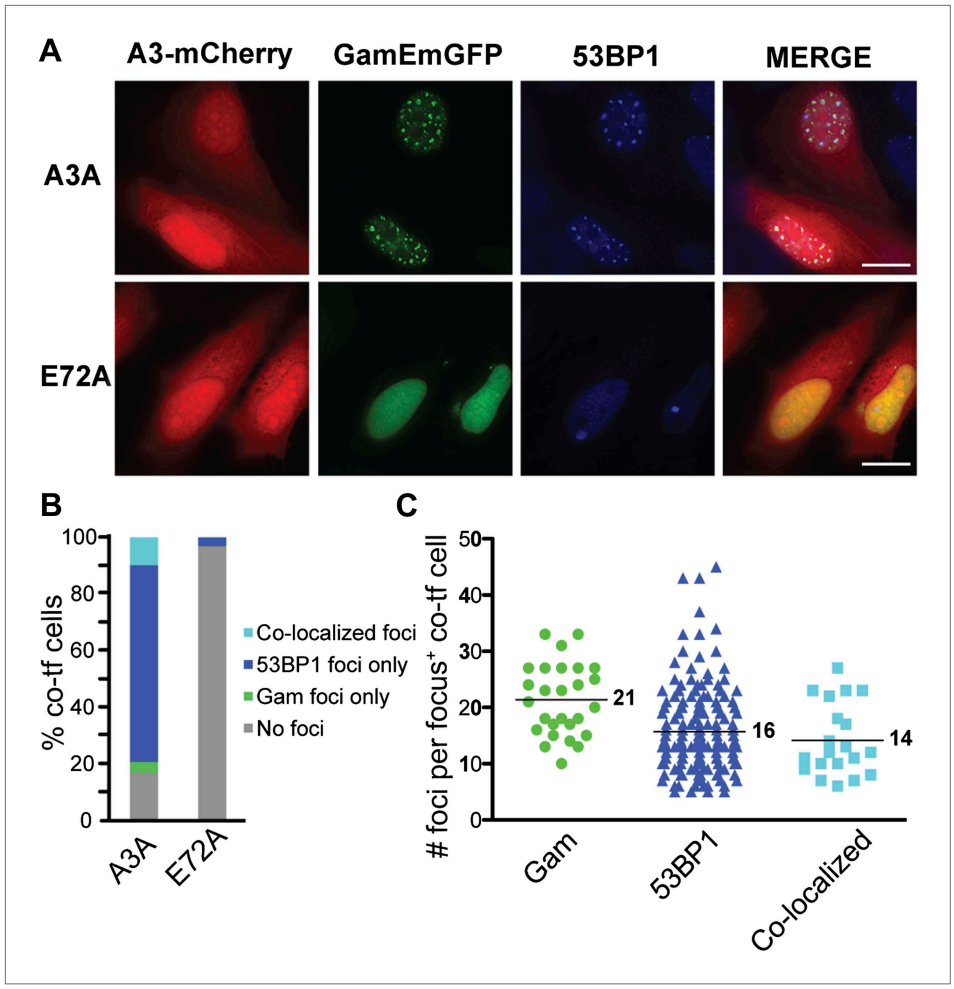

Figure 7. APOBEC3A induces DSBs in human cells. (**A**) HeLa cells co-transfected with GamEmGFP and APOBEC3A-mCherry or catalytic mutant, APOBEC3A-E72A-mCherry. (**B**) Summary of foci observed in cells producing both GamEmGFP and A3A-mCherry or A3A-E72A-mCherry (two independent experiments; n = 100 per experiment). Data are percent of co-transfected cells. (**C**) Mean number of foci per focus-positive cell co-transfected with and expressing both GamEmGFP and A3A-mCherry.

DOI: 10.7554/eLife.01222.016

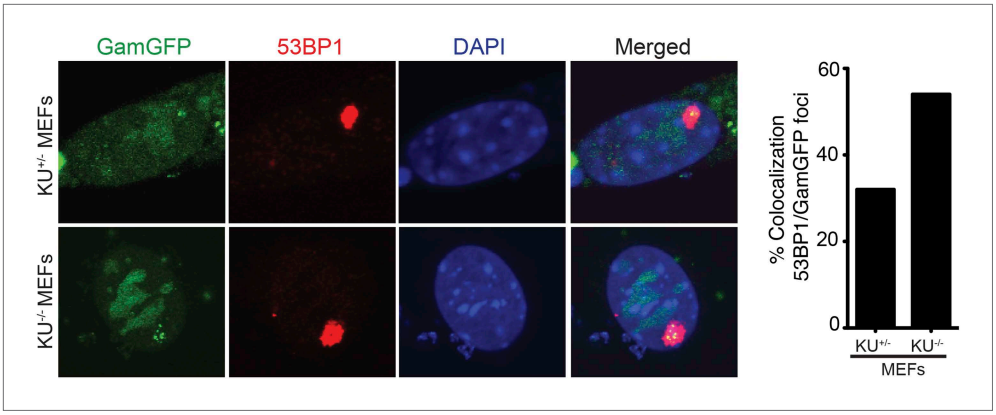

Figure 8. Spontaneous DNA breakage in G1-phase cells: GamGFP shows large spontaneous G1 53BP1 foci to contain multi-break clusters. The large spontaneous 53BP1 foci in undamaged cells, which occur solely in G1 (***Harrigan et al., 2011***; ***Lukas et al., 2011a***), contain multiple DSBs that are marked by GamGFP. The GamGFP-53BP1 co-localization is more apparent in the absence of Ku. Data are from three (Ku80-proficient) or four (Ku80-defective) independent experiments of >25 cells each with Z-stacked (optically sectioned) nuclei.

DOI: 10.7554/eLife.01222.017